Corrosion Science 63 (2012) 342–350

Contents lists available at SciVerse ScienceDirect

Corrosion Science

journal homepage: www.elsevier.com/locate/corsci

Corrosion protection of aluminium alloy by cerium conversion and conducting polymer duplex coatings

Herbert D. Johansen [a,b], Christopher M.A. Brett [b], Artur J. Motheo [a,*]

[a] Departamento de Físico-Química, Instituto de Química de São Carlos, Universidade de São Paulo, Av. Trabalhador Sancarlense 400, CP 780, CEP 13560-970, São Carlos, SP, Brazil
[b] Departamento de Química, Faculdade de Ciências e Tecnologia, Universidade de Coimbra, Rua Larga, 3004-535 Coimbra, Portugal

ARTICLE INFO

Article history:
Received 15 April 2012
Accepted 16 June 2012
Available online 23 June 2012

Keywords:
Alloy
Aluminium
Polarization
Paint coatings
Pitting corrosion
Polymer coatings

ABSTRACT

The corrosion protection of AA6063 aluminium alloy by cerium conversion, polyaniline conducting polymer and by duplex coatings has been investigated. The electrochemical behaviour was evaluated in aerated 3.5 wt.% NaCl. All coatings tested shifted the corrosion and pitting potentials to more positive values, indicating protection against corrosion. The duplex coatings are significantly more effective than each coating alone: corrosion and pitting potentials were shifted by +183 and +417 mV(SCE), respectively, by duplex coatings in relation to the untreated aluminium alloy. Optical microscopy and scanning electron microscopy are in agreement with the electrochemical results, reinforcing the superior performance of duplex coatings.

1. Introduction

Aluminium alloys have been the choice material for aircraft construction since the 1930s [1]. The aerospace industry relies heavily on AA2xxx (Al–Cu–Mg) and AA7xxx (Al–Zn–Mg) aluminium alloy series, while AA6xxx (Al–Mg–Si) aluminium alloys are of particular interest nowadays. To AA6xxx aluminium alloys magnesium and silicon are added in appropriate proportion to form Mg_2Si, which is a basis for age hardening on these alloys, giving them numerous benefits including medium strength, formability, weldability and low cost. They can be used in a variety of applications, after appropriate heat treatment, including aircraft fuselage skins and automobile body panels and bumpers, instead of more expensive AA2xxx and AA7xxx alloys [2]. However, since the corrosion properties of these aluminium alloys vary, there is a need for studies of different methods of corrosion protection. The use of protective coatings reduces the corrosion rate and extends the useful life of these materials.

Protection against corrosion usually involves chemical or electrochemical treatments that can incorporate a conversion coating or anodizing before the application of other coatings [3]. The corrosion resistance of aluminium alloys has been enhanced by the use of chromating, which is still the most commercially used surface pre-treatment. The major reasons for the widespread use of chromium protective coatings are their self-healing nature, excellent corrosion resistance and ease of application. However, current environmental legislation means total exclusion of Cr^{VI} in the near future due to its toxic nature, so there is a need to develop non-toxic alternative methods of corrosion protection [4]. Consequently, research into alternative non-toxic corrosion inhibitors has led to the development of various novel conversion coating processes [5–14]. Recent patents cover a variety of new coating formulations [15–18].

Hinton et al. [19] proposed the use of electroless conversion coatings on aluminium alloys deposited from solutions containing salts of rare earth elements. From this work, Hinton and co-workers [20,21] investigated the use of compounds of lanthanide elements as conversion coatings on different aluminium alloys. The oxides of rare earth elements were found to provide effective corrosion protection. They control the cathodic reaction associated with the increase of pH due to oxygen reduction by localised precipitation of metal hydroxides. Of the rare earth compounds, cerium shows maximum corrosion protection efficiency. An important reason for the superior efficiency of cerium is due to Ce^{IV}, which can be formed in high pH value environments [22].

Aldykewicz et al. [23] reported that corrosion inhibition by $CeCl_3$, added to NaCl solution, is related to the development of a cerium-rich layer on copper cathode sites on the AA2024 aluminium alloy surface. Mishra et al. [24] investigated the inhibitory effect of $LaCl_3$ and $CeCl_3$ added to NaCl solution against corrosion of AA2014 aluminium alloy, concluding that, for all the concentrations studied, $CeCl_3$ was the better corrosion inhibitor. Decroly and Petitjean [25] applied cerium conversion coatings on AA6082 aluminium alloy, studying the pre-treatment effect and observed

* Corresponding author. Tel.: +55 16 3373 9932; fax: +55 16 3373 9952.
E-mail address: artur@iqsc.usp.br (A.J. Motheo).

0010-938X/$ - see front matter © 2012 Elsevier Ltd. All rights reserved.
http://dx.doi.org/10.1016/j.corsci.2012.06.020

that the addition of a small quantity of $CuCl_2$ as catalyst improves the adhesion of the cerium conversion coatings. Salazar-Banda et al. [26] investigated the anticorrosion efficiency of cerium-based coatings prepared by the sol–gel method. They demonstrated that direct application of ceramic cerium-based sol–gel coatings on AA7075 aluminium alloy substrates produces high-performance anticorrosion layers. Electrochemical experiments and analyses of the microstructure demonstrate that the protective cerium-based layers are very efficient for passivation of the alloy surface, operating as both passive and active barriers for corrosion protection.

The other most widespread strategy for corrosion protection is the application of polymer coatings, which cover the protected surface mechanically as a dense barrier against corrosive agents. Conducting polymer films have been suggested as having advantages over polymers which present a purely physical barrier, since they can confer anodic or cathodic protection, although which of these depends on the polymer and the solution conditions. Since DeBerry's pioneering work on steel corrosion protection by polyaniline (PAni) films [27], the performance of such kinds of coatings has been tested on different materials.

PAni is constituted by oxidised and reduced segments with different ratios [28–32]. Thus, PAni can be in the reduced and oxidised forms, leucoemeraldine and pernigraniline, respectively, or, in the case of an equal content of both segments, one gets the emeraldine form. Emeraldine base (EB) is a non-conductive form and has to be doped to become conductive, which can be performed by using protonic acids and creating p-charge carriers. The protonation results in relatively stable radical cations that are responsible for the electrical conductivity, with their charges being compensated by the respective anions to obtain the emeraldine salt (ES). The emeraldine–leucoemeraldine reversible transition plays an important role in corrosion protection of metals by passivation [28], inducing a significant potential shift towards more positive values and an increase of the polarization resistance [29]. In addition, PAni increases corrosion protection through its barrier and permeable-selective properties, i.e., high diffusion resistance toward corrosive ions, particularly in the case of undoped emeraldine.

A recent review points out that despite extensive research, mainly on steels, challenges remain as to how to test these polymers in situations similar to those encountered in practice [30]. Recent examples on stainless steels include passivation by PAni coatings in acid solution [31] and with two different incorporated counter ions [32]. The passivating ability of PAni was exploited on mild steel by incorporating it in epoxy-coal tar coatings [33].

PAni-based organic inhibitors and derivatives have also been extensively used for the protection of aluminium alloys e.g. [34–39]. Huerta-Vilca et al. [36] investigated PAni electrodeposition on AA1050 aluminium alloy (99.50 wt.% Al) and studied the anodic activation of alloy surface in nitric acid solution containing aniline to obtain a porous surface containing pits filled with PAni [37]. The most interesting aspect in the mechanism of corrosion protection by PAni is its ability to repair defects in oxide layers that naturally recover the material, maintaining its integrity and natural corrosion protection character. The anodic protection of AA5182 alloy was successfully explained by galvanic coupling with the substrate [40]. The polymer layer also acts as a barrier between the corroding species and the metal surface. Silva et al. [41] reported the electrochemical behaviour of AA2024 aluminium alloy modified with self-assembled monolayer/PAni duplex films. They concluded that the best protection against corrosion is probably due to anodic protection associated with the barrier effect. On other hand, if the barrier is non– or partially adherent on the surface the coating itself cannot stop the corrosion. So, the development of protective systems to improve the adherence of these conducting polymers and to study the corrosion inhibition effect of these systems is important. Duplex films using PAni and cerium on aluminium alloys were already reported by Kamaraj et al. [42], depositing the conducting polymer on the alloy surface followed by a post-treatment in a hot cerium salt solution. The authors claim that the corrosion protection is improved by the presence of Ce^{III} and Ce^{IV} on the polymer surface. Very recently, Kartsonakis et al. [43] developed hybrid organic–inorganic multilayer coatings for the corrosion protection of AA2024 aluminium alloy. The alloy was coated with two layers, the first consisting of a coating of polyaniline–polypyrrole copolymer including CeO_2 nanocontainers loaded with 2-mercaptobenzothiazole and the second upper one of an oxysilane-based sol–gel coating. The multilayer coatings were tested for their protection against corrosion using electrochemical techniques; however, nothing was said about the adherence of this novel system.

The aim of this work is to investigate the electrochemical behaviour of a duplex coating constituted by a cerium conversion coating, as adherence promoter, and PAni in the corrosion protection of AA6063 aluminium alloy.

2. Experimental

2.1. Substrate preparation

The AA6063 aluminium alloy has the following elemental composition (wt.%): 0.20–0.6 Si, 0.35 Fe, 0.10 Cu, 0.10 Mn, 0.45–0.9 Mg, 0.10 Cr, 0.10 Zn, 0.10 Ti, 0.15 other elements and balanced with Al. Coupons of AA6063 were cut and mechanically abraded with abrasive paper (100–1200 mesh), cleaned with ethanol, rinsed in water and dried for tests. The final surface aspect of the coupons was the same as the aluminium alloy finish for industrial applications.

2.2. Cerium conversion coating

Aluminium alloy coupons were pre-treated by immersing them in 1.25 mol L^{-1} NaOH aqueous solution during 5 min at room temperature and rinsing with water prior to deposition. The cerium conversion coating was obtained by immersion of the alkaline pre-treated samples in a solution containing 5 mmol L^{-1} $Ce(NO_3)_3{\cdot}6H_2O$, pH 4.0 (adjusted with HNO_3), and 10 mL L^{-1} 30 wt.% H_2O_2. The temperature was kept at 25 ± 2 °C and after a 10 min electroless deposition, the samples were rinsed with water and dried. After this process the samples were called Ce-coated.

2.3. PAni and duplex coatings

For the conducting polymer coating, a saturated PAni solution was obtained by adding 7 g of undoped PAni (chemically synthesized [44]) to 100 mL of *N*-methyl-pyrrolidone and irradiating with

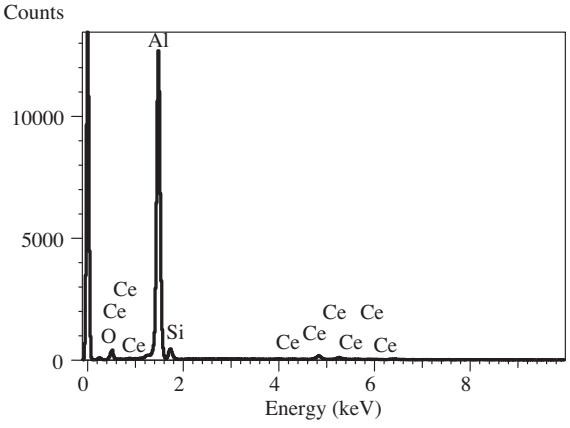

Fig. 1. EDS spectrum of Ce-coated AA6063 aluminium alloy surface. Analysed area: 2.16×10^{-3} cm^2. Resolution: 112 eV.

ultrasound for 10 min for complete dissolution. The bare samples were then painted using a paint brush with the PAni casting solution and dried at 50 °C under vacuum, obtaining coatings with less than 40 μm thickness. The samples submitted to this process were called PAni-coated samples. The duplex coatings were obtained by combining the two procedures, i.e. the application of PAni solution on a surface previously covered by a cerium deposit.

2.4. Coating characterization

Optical micrographs were obtained using an optical microscope LEICA model DFC-208 coupled to an image acquisition system. SEM images were obtained using a scanning electron microscope ZEISS-LEICA model 440, operated with electron beams of 20 kV. Analyses of the cerium conversion coating composition were performed by energy dispersive X-ray spectroscopy (EDS) with an X-ray dispersion spectrometer, OXFORD 7060 with resolution of 112 eV.

2.5. Electrochemical measurements

Measurements were carried out in a single-compartment electrochemical cell. The open circuit potential (OCP) and polarization curves, at 1 mV s^{-1}, were obtained in aerated 3.5 wt.% NaCl solution. A potentiostat/galvanostat EG&G/PAR model 273-A controlled by EG&G/PAR M352 software was used for the electrochemical tests. A three-electrode flat corrosion cell was used, containing the AA6063 aluminium alloy specimens as working-electrode, a Pt foil as counter-electrode and a saturated calomel electrode (SCE) as reference. All electrochemical experiments were performed at 25 ± 2 °C.

2.6. Salt spray tests

Accelerated corrosion tests were carried out using rectangular AA6063 aluminium alloy specimens (2.0 × 2.5 × 0.5 cm) in a salt

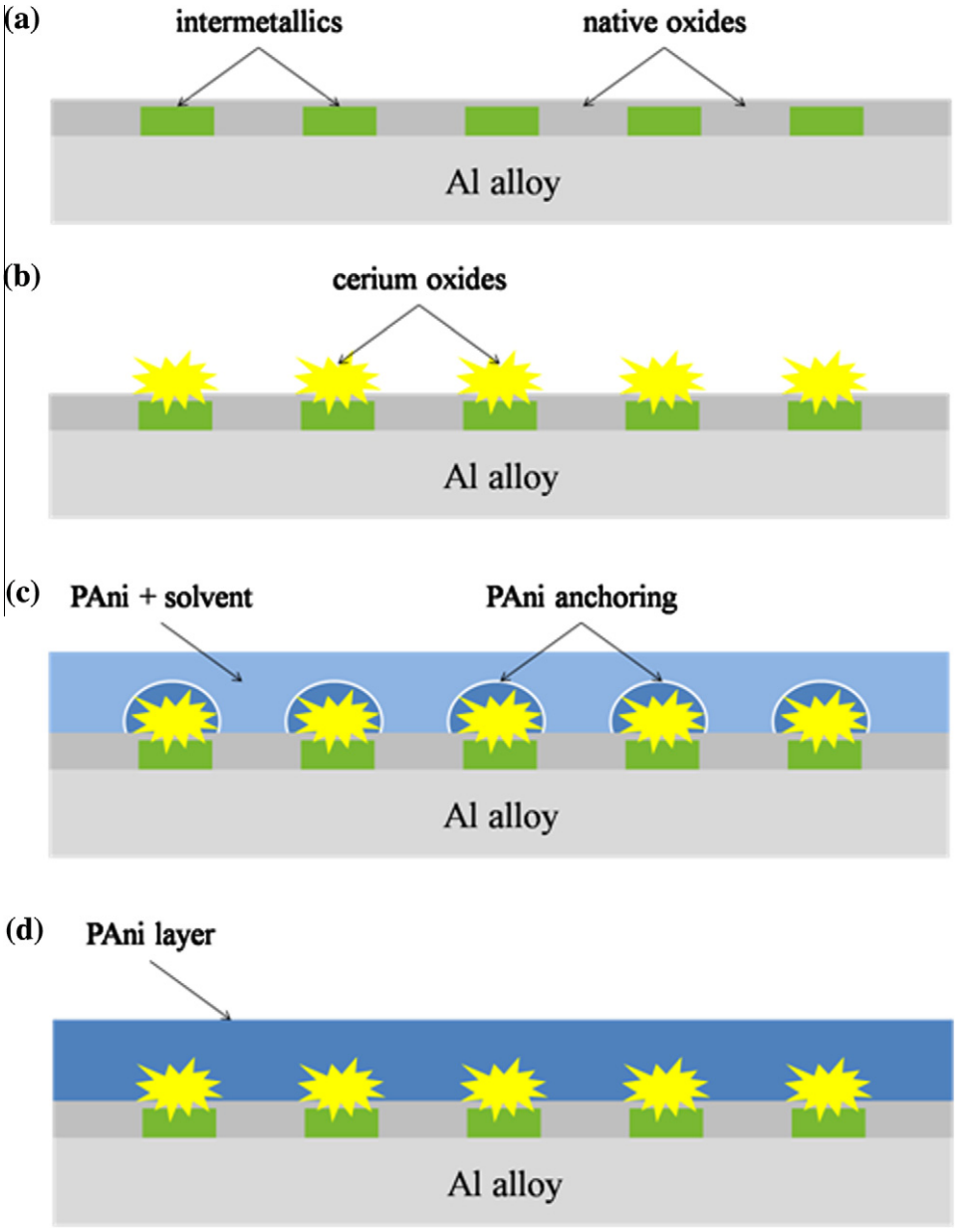

Fig. 2. Illustrative scheme of a duplex coating on the AA6063 aluminium alloy surface. The duplex coating consists of a PAni layer on the top of electroless deposited cerium coating: (a) aluminium alloy with intermetallic region and native oxides, (b) after cerium electroless deposition, (c) initial PAni anchoring on the modified intermetallic region and (d) PAni layer after solvent evaporation, representing the final treatment stage for the duplex coating.

spray chamber BASS model CTT-LQ. The samples were exposed for 240 h using 5 wt.% NaCl solution (6.5 < pH < 7.2) with a spray flow rate of 40 mL h^{-1}, according to standard ASTM B117-07a [45]. During the tests the chamber was kept at 35 ± 1 °C. Periodically the samples were removed from the chamber for visual evaluation of the extent of corrosion. The coating inhibitor efficiency was assessed visually by comparing the size of the corroded area before and after the tests.

2.7. Determination of adhesion

The adhesion of the PAni coatings was assessed by the Brazilian ABNT NBR 11003 standard [46], a method for the determination of the adhesion of paints and varnishes, equivalent to ASTM D3359-09e2 standard test method. For this purpose, Scotch 880 3M adhesive tape was applied over a chosen area and removed by pulling it firmly at an angle close to 180 degrees. The area was checked for PAni stripping, and the adherence classified according to the following scale: 0 (no area detached); 1 (0–5%); 2 (5–15%); 3 (15–35%); 4 (35–65%) and 5 (>65% area detached). In the case of intermediate situations with non-uniform stripping, the less adherent (high level) was always considered.

3. Results and discussion

3.1. Cerium deposition

Deposition of cerium conversion coatings was carried out using the electroless method, without an applied potential or current. The conditions adopted (see Section 2) are the optimised conditions, obtained from various studies and tests to obtain the best conditions in the bath for deposition of cerium conversion coatings on AA6063 aluminium alloy surface individually and with PAni. These variables are also the subject of different studies in the literature [47–55], which confirm the strong influence of bath parameters on the characteristics of cerium conversion coatings on aluminium alloys and their effects on corrosion protection.

Fig. 1 shows an EDS spectrum of Ce-coated aluminium alloy surface (analysed area 2.16×10^{-3} cm^2) in which there is a peak corresponding to Al with intensity close to 13,000. Analysis indicates that the cerium composition is 7.93 wt.% and is distributed uniformly over the entire surface of the AA6063 aluminium alloy coupon. By reducing the surface area under analysis, the intensity of the peaks decreases. In particular, the peak corresponding to aluminium decreases by 35%. This observation corresponds to the latter stage of the model proposed Campestrini et al. [50] when the entire surface is covered with a layer of cerium, which blocks the weak signal of the intermetallic particles surrounded by aluminium.

The deposition can be divided into two stages as described by Hughes et al. [52]: (i) a period of induction, which is activation of the substrate followed by aluminium oxide growth on the matrix and (ii) a period of deposition, which essentially involves the deposition of cerium hydroxides on the aluminium matrix, and continued activation around the previously active sites [52–54].

From these experiments it was found that formation of the cerium conversion coating must be preceded by surface treatment in alkaline medium so that intermetallic constituents present in the aluminium alloy can emerge onto the surface. The importance of these intermetallic particles is the fact that they take part in the OH^- ion generation mechanism, through decomposition of H_2O_2 in the electroless conversion bath [50]. If these intermetallic particles are absent, the cerium conversion coating deposition is not favoured. However, cerium conversion coatings are formed on the AA6063 aluminium alloy for the compositions investigated, but not so thick on the surface as in other methods [26] or when using other cerium salts [22,47,55]. Thus, the amount of cerium used, the dispersion of deposits on the surface and the formation of anchor points (around 0.44 μm thickness) for the subsequent deposition of PAni are important factors.

The cerium conversion coating process leads to a rough surface which provides, besides improvement in the adherence of PAni on the substrate (duplex coatings), better corrosion protection compared to bare AA6063 alloy. A scheme illustrating a possible arrangement in a duplex coating is shown in Fig. 2, representing the final treatment stage for the duplex coating. For the cerium conversion coating, the model of Campestrini et al. [50] is applicable given that involves initial thinning of the native oxide on the aluminium alloy surface. For PAni coated on the bare substrate, low adhesion to the surface was evident.

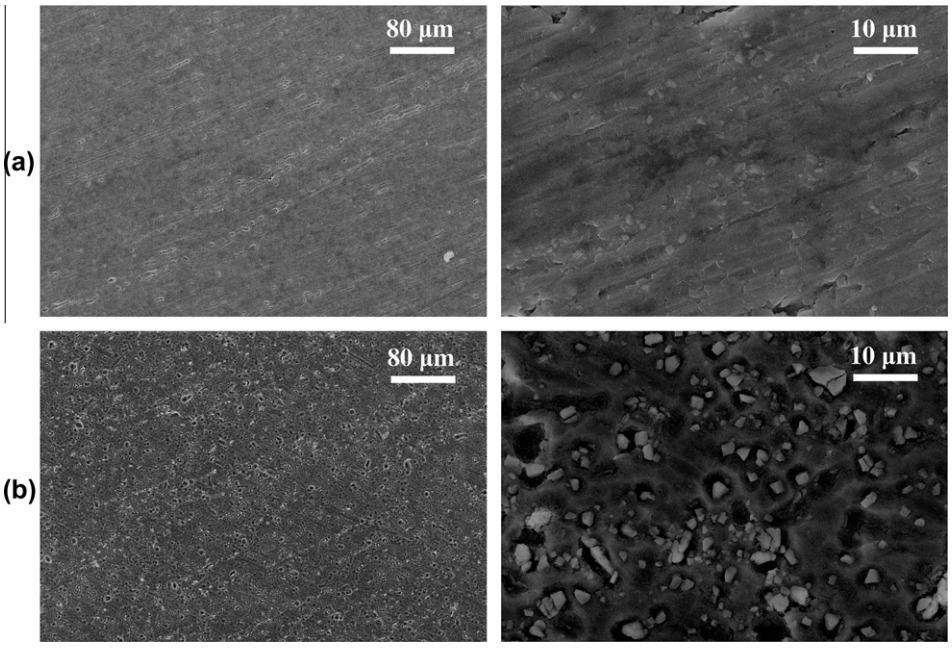

Fig. 3. SEM images of AA6063 aluminium alloy: (a) bare and (b) Ce-coated.

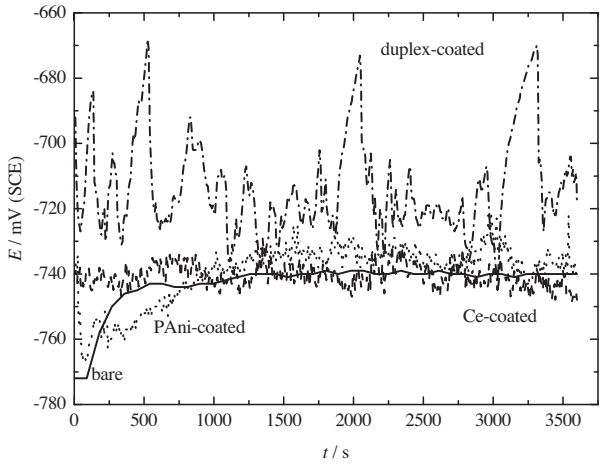

Fig. 4. Open circuit potentials of AA6063 aluminium alloy and with different coatings in aerated 3.5 wt.% NaCl.

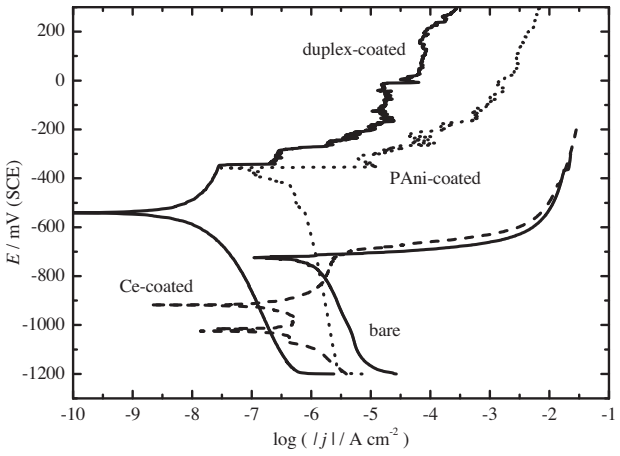

Fig. 5. Polarization curves for the AA6063 aluminium alloy specimens with different coatings in aerated 3.5 wt.% NaCl. Scan rate 1 mV s^{-1}.

Fig. 3 shows SEM micrographs of AA6063 coupons of an abraded, bare surface and coated with cerium. It is clear that the surface roughness increases homogeneously (a yellowish colour can be observed over the entire surface) that is one of the important factors to improve the adherence of the polymer films subsequently deposited on the surface. In the Ce-coated aluminium alloy surface, some particles are observed (white spots with regular edges) that were not analysed or identified at this time.

3.2. Open circuit potential (OCP)

The dependence of open circuit potential with time for uncoated and coated AA6063 aluminium alloy samples immersed in aerated 3.5 wt.% NaCl solution, obtained before recording the polarization curves, are shown in Fig. 4. In such an aggressive environment, corrosion processes generally lead to the formation of a passivating oxide layer. The open circuit potential value of the duplex coated sample is more positive than that of the bare AA6063 aluminium alloy after 1 h of immersion. This behaviour does not mean greater corrosion protection but it does indicate that the PAni film on the top of the cerium deposit has a sufficiently good adherence to shift the OCP to a more positive value [36].

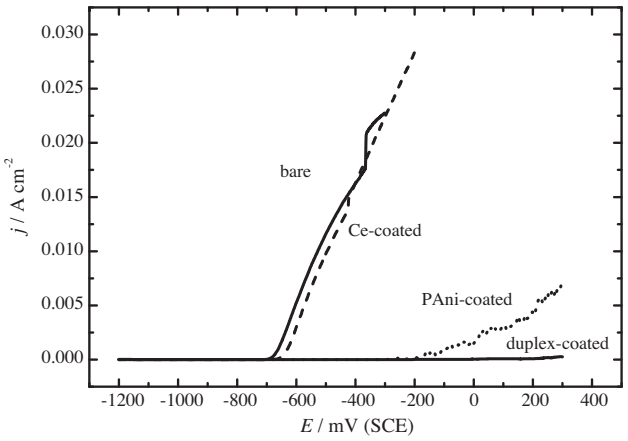

Fig. 6. Linear scan voltammetry for the AA6063 aluminium alloy specimens with different coatings in aerated 3.5 wt.% NaCl. Scan rate 1 mV s^{-1}.

3.3. Potentiodynamic curves

Polarization curves of the AA6063 aluminium alloy with their respective coatings, in aerated 3.5 wt.% NaCl solution, are shown in Fig. 5. At negative potentials near the corrosion potential, the cathodic reaction rate is reduced when the cerium conversion coating is present, compared to the bare alloy. To obtain the corrosion parameters from the curves in Fig. 5, the EG&G/PAR M352 ParCalc software was used to obtain the Tafel coefficients (β_a and β_c), polarization resistances (R_{pol}) and corrosion current densities (j_{cor}) (Table 1). The determination starts by selecting two data points from the cathodic and anodic branches in polarization curves, at potential regions between +50 mV and −50 mV with respect to E_{cor}. As a rule for an accurate procedure to obtain the corrosion parameters, the branches selected of the polarization curves should exhibit Tafel behaviour over at least half decade of current density. If not adopted this criteria, a poor selection of the points to be used can change the corrosion current density significantly. There are several factors that can lead to non-ideal Tafel behaviour. The diffusion limitations on a reaction, for example by PAni barrier effect (PAni and duplex-coated), and ohmic losses in solution can lead to a curvature of the Tafel region, leading to erroneously high estimation of corrosion current density. Nevertheless, the good fitting accuracy was confirmed by chi-square (χ^2) values less than 1.56×10^{-10}. Additionally, the protection efficiency (P), in percent, can be calculated from the polarization measurements by the expression [56]:

$$P = \left(1 - \frac{R_{ps}}{R_{pc}}\right) \times 100 \quad (1)$$

where R_{ps} and R_{pc} are the polarization resistances of the bare and modified surfaces, respectively.

Table 1
Electrochemical parameters obtained from the polarization curves of AA6063 aluminium alloy.

	OCP/mV(SCE)	E_{cor}/mV(SCE)	j_{cor}/A cm^{-2}	β_a/mV dec^{-1}	$-\beta_c$/mV dec^{-1}	R_{pol}/Ω cm^2	E_{pit}/mV(SCE)	P/%
Bare	−740	−725	1.1×10^{-6}	19	610	8.01×10^3	−690	–
Ce-coated	−748	−918	1.0×10^{-7}	53	71	8.80×10^5	−662	99.1
PAni-coated	−738	−351	1.5×10^{-7}	26	550	7.78×10^4	−280	89.7
Duplex-coated	−718	−542	5.9×10^{-9}	193	259	5.57×10^7	−273	99.9

According to Table 1, the duplex coating shifts the values of corrosion potential (E_{cor}) and pitting potential (E_{pit}) by +183 mV(SCE) and +417 mV(SCE) respectively, in relation to the bare AA6063 aluminium alloy. The cathodic and anodic branches of the polarization curves both show lower values of current density compared to the untreated alloy.

When hydrated oxides of cerium are formed on the aluminium alloy surface in addition to aluminium oxide, a barrier to the flow of electrons can be created. This can reduce the rate of oxygen reduction and inhibit corrosion. In the case of the duplex-coated sample, the currents are even lower.

Typically, the oxides of lanthanide elements are characterised by a high electrical resistivity [51] and the presence of cerium oxide films causes a decrease in reaction rate for oxygen reduction on the surface of aluminium alloys as well as of metal oxidation. As a result, both cathodic and anodic branches of the curves are

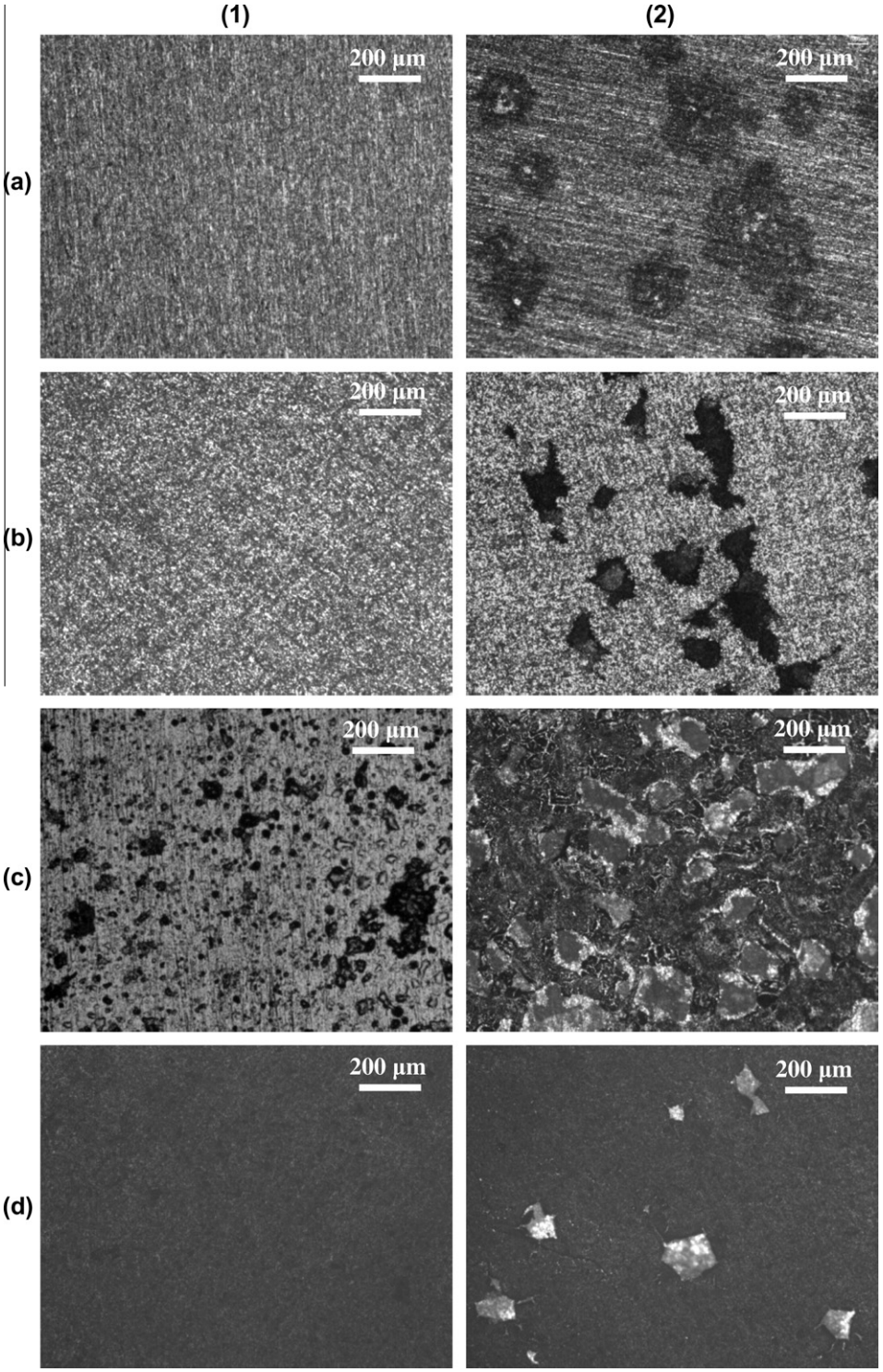

Fig. 7. Optical micrographs of AA6063 aluminium alloy specimens (1) before and (2) after electrochemical tests: (a) bare; (b) Ce-coated; (c) PAni-coated and (d) duplex-coated.

shifted towards lower values of current density. The values of P in Table 1 reflect the effects of the different factors relating to surface protection against corrosion. The PAni-coated surface gives poor protection efficiency because of the low adherence of the PAni film whilst the duplex coating leads to more than 99.9% efficiency.

Fig. 6 shows polarization curves starting from the potential value where E_{pit} values were obtained, normalising, at this potential value, the current density to zero. It is observed that the tendency for localised corrosion to occur is also decreased by duplex coatings, since the value of the pitting potential becomes more positive. However, this feature cannot be extrapolated to the PAni coatings. Furthermore, although E_{cor} is shifted to more positive values, the decrease of corrosion current density is not significant. Possibly, the low adherence of PAni allows solution to penetrate through the coating, increasing the corrosion rate under the PAni coating, the fact that there is formation of bubbles and deformation of

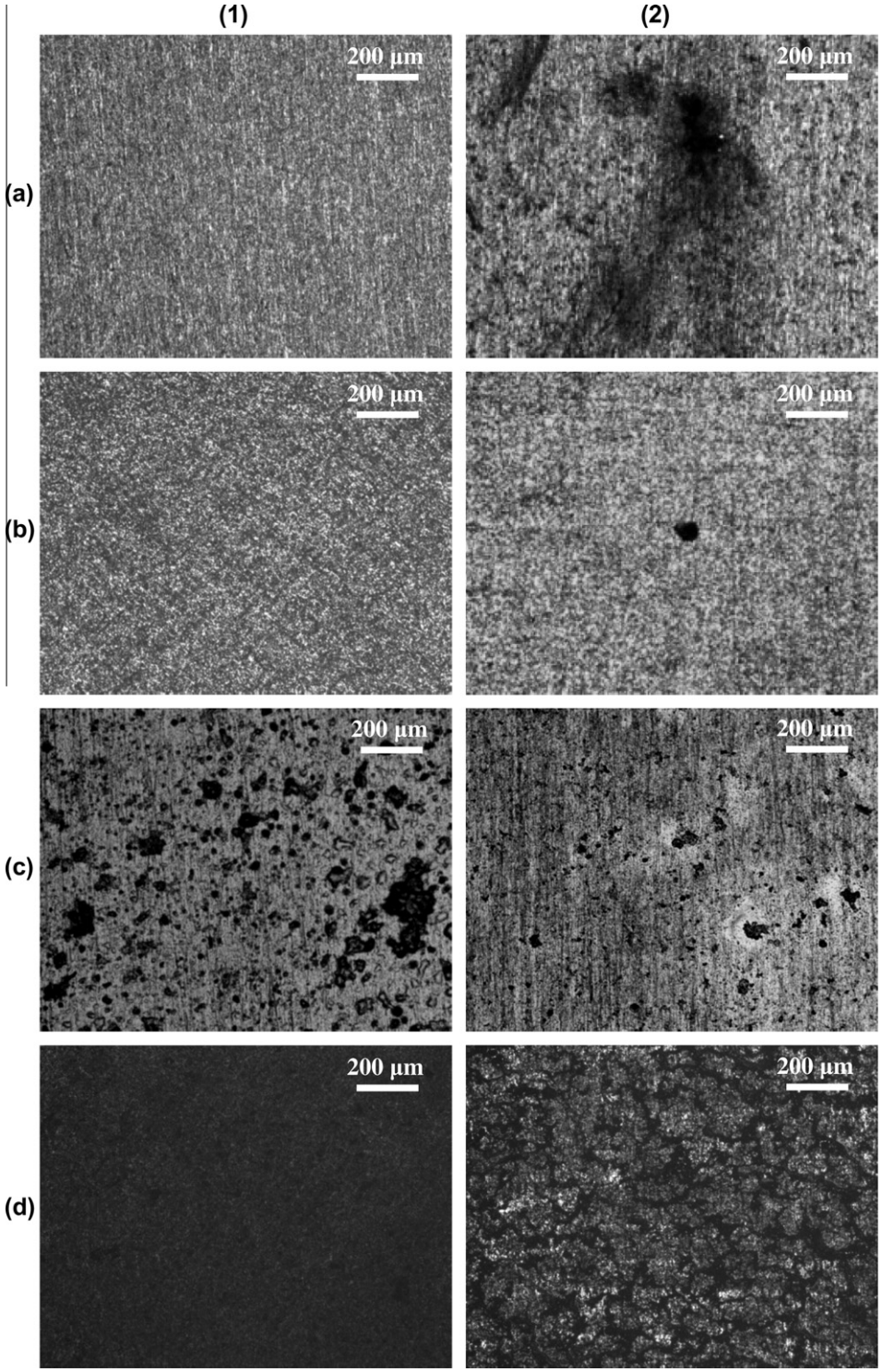

Fig. 8. Optical micrographs of AA6063 aluminium alloy specimens (1) before and (2) after 240 h in salt spray chamber: (a) bare; (b) Ce-coated; (c) PAni-coated and (d) duplex-coated.

the conducting polymer coating supporting this hypothesis. The optical micrographs in Fig. 7, obtained before and after the potentiodynamic tests, show that, after the tests, the bare surface presents some dark spots distributed homogeneously while the Ce-coated surface presents non-uniformly distributed, smaller spots of irregular shape, attributed to imperfections of the surface. On the other hand, the PAni-coated surface already had many small dark points before the tests were done, that increase in size during the electrochemical experiments. This behaviour can be related to the low adherence of the PAni coating on the surface. Finally, the duplex-coated surface presented a smooth aspect before and after the tests except for a few cracks in the PAni layer, not distributed over the whole surface. These observations are in agreement with the electrochemical results, reinforcing the superiority of duplex coatings as corrosion protection systems with a smaller tendency to degradation under polarization.

3.4. Salt spray test

Exposure to salt spray during 240 h drastically alters the appearance of the coatings on the AA6063 aluminium alloy surface, as seen in Fig. 8. Nevertheless, at the end of this time some coating is still left on the surface, attached to the metal substrate, but the surfaces are significantly altered with the appearance of cracks in the outer layer of the duplex coatings or localised corrosion without corrosion products (Ce-coated and PAni-coated) and with corrosion products (bare alloy). The cracks in the PAni of the duplex-coated sample shows that the PAni film remains on the surface after the salt spray test, since the cerium conversion coating promotes the anchoring of the PAni coating.

The salt spray test shows that: (i) formation of cerium conversion coatings promotes greater stability of PAni and its anchorage is favoured in the AA6063 aluminium alloy duplex coatings; (ii) cerium conversion coatings are resistant to deterioration when exposed to salt spray; (iii) the aluminium alloy coated with the duplex coating is corroded at a lower rate than with cerium or PAni coatings individually.

3.5. Determination of adhesion

One of the most important properties of the coatings is their adhesion to the substrate and most of the corrosion resistance characteristics are linked to adhesion properties [57]. If the coating has unsatisfactory adhesion to the substrate, its performance will be compromised.

Adhesion tests for the samples coated with PAni films were carried out according to ABNT NBR 11003 [46], for the determination of adhesion of paints and varnishes, in which 0 is considered a high adhesion and 5 a low adhesion. The adherence factors are 1 for duplex and 3 for PAni coatings. This trend is in agreement with the other types of experiment, with the duplex coating presenting more adherence than the coating of PAni by itself.

The results of accelerated corrosion tests and the determination of adherence showed that the AA6063 aluminium alloys with PAni coatings are useful alone for corrosion protection. However, the duplex coatings have a greater potential for protection against corrosion, since they showed a better performance in the tests that were carried out.

4. Conclusions

The cerium conversion, PAni and duplex protective coatings studied in the present work all shift the values of corrosion and pitting potentials to more positive values indicating corrosion protection. Among the coatings analysed, duplex coatings are significantly more effective than single cerium conversion or PAni coatings, the trend in corrosion potential being: Ce-coated < PAni-coated < duplex-coated. Additionally, duplex coatings decrease the values of corrosion current density indicating that the corrosion rate also decreases. Salt spray tests, adherence tests and optical microscopy are in agreement with the electrochemical results. For the cerium electroless deposits on AA6063 it is important that the deposition is preceded by surface treatment in alkaline medium so that intermetallic constituents can emerge on the surface, providing active redox sites. Following a model proposed in the literature, once the cerium deposition starts, the deposits will grow bi-dimensionally until their coalescence, which will lead to the entire surface being covered. This resulting surface is rough and electrochemically active, providing all the conditions of anchorage and reactivity necessary for the formation of adherent PAni films.

For the duplex coating the general corrosion protection mechanism has two contributions: (i) the cerium coating acting as a barrier and (ii) the conducting polymer presenting anodic protection associated with a barrier effect. Finally, the presence of a cerium conversion coating was seen to improve the adherence of the PAni films on the AA6063 surface and, at the same time, has an important protective character that improves the duplex coating performance. In future work, reduction of the amount of deposited cerium will be investigated with a view to increasing the economic viability of the proposed protection scheme.

Acknowledgements

The authors wish to thank the Brazilian funding agencies CNPq [140402/2009-8 and 160466/2011-3] and CAPES [BEX 4935/10-1] for the Grants conceded and the Portuguese funding agency FCT [CEMUC® (Research Unit 285)].

References

[1] E. Tan, B. Ögel, Turkish J. Eng. Environ. Sci. 31 (2007) 53–60.
[2] L.P. Troeger, E.A. Starke, Mater. Sci. Eng. A 277 (2000) 102–113.
[3] J.D. Gorman, A.E. Hughes, D. Jamieson, P.J.K. Paterson, Corros. Sci. 45 (2003) 1103–1124.
[4] J.O. Stoffer, T.J. O'Keefe, L. Xuan, E. Morris, P. Yu, S.P. Sitaram, Inventors. United States patent USP 5,932,083, 1999.
[5] K. Horn, S. Krause, G. Weinberg, K. Bange, Thin Solid Films 150 (1987) 41–50.
[6] H. Konno, J. Electrochem. Soc. 134 (1987) 1034–1035.
[7] H. Bubert, H. Puderbach, H. Pulm, W.A. Roland, Fresenius Z. Anal. Chem. 333 (1989) 304–307.
[8] D.R. Arnott, B.R.W. Hinton, N.E. Ryan, Corrosion 45 (1989) 12–18.
[9] G. Goeminne, H. Terryn, J. Vereecken, Electrochim. Acta 40 (1995) 479–486.
[10] T. Schram, G. Goeminne, H. Terryn, W. Van Hoolst, P. Van Espen, Trans. Inst. Metal Finishing 73 (1995) 91–95.
[11] C. Monticelli, F. Zucchi, G. Brunoro, G. Trabanelli, J. Appl. Electrochem. 27 (1997) 325–334.
[12] L. Fedrizzi, F. Deflorian, P.L. Bonora, Electrochim. Acta 42 (1997) 969–978.
[13] L. Fedrizzi, F. Deflorian, S. Rossi, in: Proceeding of the Conference on Aluminium Surface Science and Technology, Antwerp, 1997, pp. 243–247.
[14] V. Subramanian, W.J. van Ooij, Surf. Eng. 15 (1999) 168–172.
[15] L.S. Sander, E.M. Musingo, W.J. Neill, Inventors. United States patent USP 4,921,552, 1990.
[16] N. Das, Inventor. United States patent USP 5,139,586, 1992.
[17] R.N. Miller, Inventor. United States patent USP 5,356,492, 1994.
[18] C.E. Tomlinson, Inventor. United States patent USP 5,380,374, 1995.
[19] B.R.W. Hinton, D.R. Arnott, N.E. Ryan, Metals Forum 7 (1984) 211–217.
[20] B.R.W. Hinton, D.R. Arnott, N.E. Ryan, Metals Forum 9 (1986) 162–173.
[21] D.R. Arnott, N.E. Ryan, B.R.W. Hinton, B.A. Sexton, A.E. Hughes, Appl. Surf. Sci. 22–23 (1985) 236–251.
[22] K.A. Yasakau, M.L. Zheludkevich, O.V. Karavai, M.G.S. Ferreira, Prog. Org. Coat. 63 (2008) 352–361.
[23] A.J. Aldykewicz, H.S. Isaacs, A.J. Davenport, J. Electrochem. Soc. 142 (1995) 3342–3350.
[24] A.K. Mishra, R. Balasubramanian, Corros. Sci. 49 (2007) 1027–1044.
[25] A. Decroly, J.P. Petitjean, Surf. Coat. Technol. 194 (2005) 1–9.
[26] G.R. Salazar-Banda, S.R. Moraes, A.J. Motheo, S.A.S. Machado, J. Sol–Gel Sci. Technol. 52 (2009) 415–423.
[27] D.W. DeBerry, J. Electrochem. Soc. 132 (1985) 1022–1026.
[28] N. Ahmad, A.G. MacDiarmid, Synth. Met. 78 (1996) 103–110.
[29] R. Racicot, R. Brown, S.C. Yang, Synth. Met. 85 (1997) 1263–1264.

[30] M. Rohwerder, Int. J. Mater. Res. 100 (2009) 1331–1342.
[31] J. Fang, K. Xu, L. Zhu, Z. Zhou, H. Tang, Corros. Sci. 49 (2007) 4232–4242.
[32] A.A. Ganash, F.M. Al-Nowaiser, S.A. Al-Thabaiti, A.A. Hermas, Prog. Org. Coat. 72 (2011) 480–485.
[33] S. Sathiyanarayanan, R. Jeyaram, S. Muthukrishnan, G. Venkatachari, J. Electrochem. Soc. 156 (2009) C127–C134.
[34] D. Huerta-Vilca, S.R. Moraes, A.J. Motheo, J. Braz. Chem. Soc. 14 (2003) 52–58.
[35] D. Huerta-Vilca, B. Siefert, S.R. Moraes, M.F. Pantoja, A.J. Motheo, Mol. Cryst. Liq. Cryst. 415 (2004) 229–238.
[36] D. Huerta-Vilca, S.R. Moraes, A.J. Motheo, J. Solid State Electrochem. 9 (2005) 416–420.
[37] D. Huerta-Vilca, S.R. Moraes, A.J. Motheo, Synth. Met. 140 (2004) 23–27.
[38] D.E. Tallman, K.L. Levine, C. Siripirom, V.G. Gelling, G.P. Bierwagen, S.G. Croll, Appl. Surf. Sci. 254 (2008) 5452–5459.
[39] M.C. Yan, D.E. Tallman, S.C. Rasmussen, G.P. Bierwagen, J. Electrochem. Soc. 156 (2009) C360–C366.
[40] L. Cecchetto, D. Delabouglise, J.P. Petit, Electrochim. Acta 52 (2007) 3485–3492.
[41] D.P.B. Silva, R.S. Neves, A.J. Motheo, Mol. Cryst. Liq. Cryst. 521 (2010) 179–186.
[42] K. Kamaraj, V. Karpakam, S. Sathiyanarayanan, G. Xenkatachari, J. Electrochem. Soc. 157 (2010) C102–C109.
[43] I.A. Kartsonakis, E.P. Koumoulos, A.C. Balaskas, G.S. Pappas, C.A. Charitidis, G.C. Kordas, Corros. Sci. 57 (2012) 56–66.
[44] S.K. Manohar, A.G. Macdiarmid, A.J. Epstein, Synth. Met. 41 (1991) 711–714.
[45] ASTM American Society for Testing of Materials. ASTM B117-07a Standard Practice for Operating Salt Spray (Fog) Apparatus, 2007.
[46] ABNT Associação Brasileira de Normas Técnicas. ABNT NBR 11003 Paints and varnishes – Determination of adhesion, 2009.
[47] L.E.M. Palomino, J.F.W. Castro, I.V. Aoki, H.G. Melo, J. Braz. Chem. Soc. 14 (2003) 651–659.
[48] M. Dabalà, L. Armelao, A. Buchberger, I. Calliari, Appl. Surf. Sci. 172 (2001) 312–322.
[49] F.H. Scholes, C. Soste, A.E. Hughes, S.G. Hardin, P.R. Curtis, Appl. Surf. Sci. 253 (2006) 1770–1780.
[50] P. Campestrini, H. Terryn, A. Hovestad, J.H.W. de Wit, Surf. Coat. Technol. 176 (2004) 365–381.
[51] B.R.W. Hinton, L. Wilson, Corros. Sci. 29 (1989) 967–985.
[52] A.E. Hughes, J.D. Gorman, P.R. Miller, B.A. Sexton, P.J.K. Paterson, R.J. Taylor, Surf. Interface Anal. 36 (2004) 290–303.
[53] A.S. Hamdy, A.M. Beccaria, J. Appl. Electrochem. 35 (2005) 473–478.
[54] M. Bethencourt, F.J. Botana, M.J. Cano, M. Marcos, Appl. Surf. Sci. 189 (2002) 162–173.
[55] E.P. Banczek, S.R. Moraes, S.L. Assis, I. Costa, A.J. Motheo, Mater. Corros. 62 (2011), http://dx.doi.org/10.1002/maco.201106205.
[56] A. Romeiro, C. Gouveia-Caridade, C.M.A. Brett, Corros. Sci. 53 (2011) 3970–3977.
[57] A.J. Motheo, L.D. Bisanha, in: A.J. Motheo (Ed.), Adhesion of Polyaniline on Metallic Surfaces, Aspects on Fundamentals and Applications of Conducting Polymers, InTech, Rijeka, 2012, pp. 19–40, (Chapter 2).